EPJ manuscript No.
(will be inserted by the editor)

Stretched configuration of states as inferred from γ-ray angular distributions in ^{40}Ar+^{208}Pb neutron transfer reactions

P. Čolović[1], S. Szilner[1], L. Corradi[2], T. Mijatović[1], G. Pollarolo[3], A. Goasduff[2,4], D. Montanari[4,5], R. Chapman[6], E. Fioretto[2], A. Gadea[7], F. Haas[5], D. Jelavić Malenica[1], N. Mărginean[8], D. Mengoni[4], M. Milin[9], G. Montagnoli[4], F. Scarlassara[4], J. F. Smith[6], N. Soić[1], A. M. Stefanini[2], C. A. Ur[8], and J. J. Valiente-Dobón[2]

[1] Ruđer Bošković Institute, Zagreb, Croatia
[2] Istituto Nazionale di Fisica Nucleare, Laboratori Nazionali di Legnaro, Legnaro, Italy
[3] Dipartimento di Fisica Teorica, Università di Torino, and Istituto Nazionale di Fisica Nucleare, Torino, Italy
[4] Dipartimento di Fisica, Università di Padova, and Istituto Nazionale di Fisica Nucleare, Padova, Italy
[5] Institut Pluridisciplinaire Hubert Curien, CNRS-IN2P3, Université de Strasbourg, Strasbourg, France
[6] School of Engineering and Computing, University of the West of Scotland, Paisley, United Kingdom
[7] Instituto de Fisica Corpuscular, CSIC-Universitat de València, Valencia, Spain
[8] Horia Hulubei National Institute of Physics and Nuclear Engineering and ELI-NP, Bucharest, Romania
[9] Department of Physics, Faculty of Science, University of Zagreb, Zagreb, Croatia

July 3, 2017

Abstract. Angular distributions of γ rays for selected transitions in ^{40,41,42}Ar isotopes have been studied with the PRISMA magnetic spectrometer coupled to the CLARA γ array. These transitions were populated in Ar isotopes reached via neutron transfer in the ^{40}Ar+^{208}Pb reaction. By comparison with the shape of the experimental angular distribution of the known E2 transitions we established more firmly the spin and parity of excited states. In particular, in ^{41}Ar for the $(11/2^-)$ state through the $(11/2^-) \rightarrow 7/2^-$ transition whose structure was discussed in term of a phonon-fermion coupled state. The comparison with the expected fully aligned spin indicated that a high level of spin alignment has been reached.

PACS. 25.70.Hi Transfer reactions – 29.30.-h – 23.20.Lv

1 Introduction

Transfer reactions have been extensively used to study nuclear structure properties of states with single-particle or vibrational character, their coupling being especially important in the vicinity of closed shells [1]. It is still an open question to what extent such couplings play a role in the dominant configuration of states strongly populated in heavy ion transfer reactions. The field received recently a boost thanks to the availability of large solid-angle magnetic spectrometers coupled to large γ arrays. With these devices it was shown how multinucleon transfer reactions could be efficiently used to populate neutron-rich nuclei moderately far from the stability, with sufficient yields to make spectroscopic studies feasible. By employing fragment-γ coincidences with the PRISMA-CLARA set-up, investigations about the importance of phonon-fermion coupling for medium mass nuclei have been carried out (see e.g. Refs. [2–8] and references therein).

Fragment-γ coincident measurements allow for an unambiguous assignment of γ rays to a specific nucleus. On the other hand, due to the difficulties to obtain γ-γ coincidences, the construction of the level scheme and the interpretation of the observed γ transitions have been mainly based on systematics with neighboring nuclei and large-scale shell-model calculations. A significant help also came from the dynamic properties of transfer reactions, which, at energies close to the Coulomb barrier, maximize the transferred angular momentum due to the matching of the orbitals of the involved states [9,10], leading to higher yields for yrast and near-yrast states. In the collision, the exchange of the mass, charge, energy and angular momentum between reaction partners is mediated by the single-particle (fermion) and surface vibration (phonon) properties of the two colliding ions [11]. One thus expects that the same degrees of freedom will play an important role in the description of the states populated in these transfer reactions. These degrees of freedom have been probed in the study of the ^{40}Ar+^{208}Pb system [2, 7, 12, 13].

An extensive discussion of the states strongly populated in the neutron transfer channels has been carried out [2]. In particular, the odd Ar spectra comprise partly single particle states and partly states that involve combinations of single-particle with a collective boson. We observed a significant population of states whose structure matched a stretched configuration of the valence neutron coupled to the vibration quanta. By a close inspection of the wave-functions of the populated states, it was con-

cluded that the important contribution to the increase of the quadrupole deformation when neutrons fill the $f_{7/2}$ orbital is a narrowing of the gap between the $s_{1/2}$ and $d_{3/2}$ proton orbitals.

For a firm attribution of the character of the populated states, experimental knowledge of other observables is required. Information about the multipolarity of the transitions can be obtained via γ-ray angular distributions. This has been shown in the case of the ^{48}Ca+^{64}Ni reaction, measured at energies about twice the Coulomb barrier, where the population of highly oriented spin in multinucleon transfer reactions was evidenced [6]. The comparison with the expected fully aligned spin indicated that a high level of spin alignment, normal to the reaction plane, has been obtained in this heavy-ion transfer reaction. In the present article, by exploiting the modularity of the CLARA detector, we analyzed angular distributions for the intense γ transitions in Ar isotopes. We used the shape of the experimental angular distribution of the known $E2$ transitions as reference to assess whether the untabulated transitions populated in the same reaction display an $E2$ character. We also carefully studied the level of spin alignment manifested in the transfer reactions. In particular we focused on the $(11/2^-) \rightarrow 7/2^-$ transition in ^{41}Ar, which has been discussed in connection with phonon-fermion couplings.

2 Experiment and method

The ^{40}Ar+^{208}Pb reaction was studied by using the PRISMA spectrometer [14–16] coupled to the CLARA γ array [17]. The description of the experimental conditions have been already extensively outlined in Refs. [2, 12, 13], to which we refer for the details. For convenience we here briefly recall the main features of the set-up and the experiment.

The positive ion injector PIAVE coupled to the ALPI post accelerator of the Laboratory Nazionali di Legnaro has been used to accelerate a ^{40}Ar beam at $E_{\rm lab}$=6.4 MeV/A. The beam impinged onto a 300 μg/cm^2 ^{208}Pb target with an average current of 7 pnA. Identification of projectile-like fragments has been made with PRISMA placed in the vicinity of the grazing angle ($\theta_{\rm lab}$ = 54°). At the entrance of the spectrometer a position-sensitive micro-channel plate detector [18] provides a start signal for time-of-flight measurements and position signals. After passing through the optical elements of the spectrometer, ions enter a focal plane [19], made of a parallel plate of multiwire type, providing timing and position signals with resolutions similar to the entrance detector. At the end of the focal plane is located an array of a transverse field multiparametric ionization chambers, providing nuclear charge (via ΔE) and total energy. The described detector system gives all the necessary information for the complete ion identification, i.e. atomic number Z, mass number A, ionic charge state, and velocity vector, which is performed via an event-by-event reconstruction of the trajectory inside the magnetic elements [13, 15, 20]. The γ rays were detected with the CLARA array [17]. It consisted of 25 HPGe clover-type detectors (22 were installed in the present experiment) situated in the hemisphere opposite to PRISMA and covering an angular range of ∼100° to 180° with respect to the entrance direction of the spectrometer [17]. The total photo-peak efficiency was of the order of 3% for E_γ=1.33 MeV. Doppler correction of γ-ray energies was performed taking into account the reconstructed velocity vector in PRISMA.

The angular distributions of the strong γ transitions could be obtained by grouping the HPGe crystals in three rings with 40, 28 and 16 crystals corresponding to the average polar angle $\theta_{\rm CLARA}$=101°, 131° and 154°, respectively. A careful evaluation of the relative efficiency of each of the CLARA ring was carried out by using a ^{152}Eu source and the γ-ray intensities, corrected for this efficiency, were normalized to the one of $\theta_{\rm CLARA}$=101°. The angular distribution function depends on spin of the initial and final states, multipolarity of the transition and degree of angular momentum alignment. Here, the normalized angular distributions have been fitted with the function $W(\theta) = a_0(1+a_2P_2(cos\theta))$, where $P_2(cos\theta)$ stands for the Legendre polynomial and a_0 and a_2 are fitting parameters. The anisotropy of the angular distributions can be characterized by the coefficient $a = a_0 \times a_2$. These coefficients have been compared with calculated values for γ transitions from aligned nuclei following the prescription of Refs. [21, 22]. For the calculation, we took into account the spins of the initial and final states and the multipolarity of the transition. As already discussed, such comparison allows to estimate the degree of angular momentum alignment of the reaction fragments, i.e. the fraction of the angular momentum transferred into fragments spin normal to the plane of the reaction.

In the next section we present the analysis of the γ angular distributions for the ^{40,41,42}Ar isotopes. This analysis was made to establish more firmly the spin and parity of excited states, in particular, for the $(11/2^-) \rightarrow 7/2^-$ transition in ^{41}Ar and to some extent for the $(6^+) \rightarrow (4^+)$ transition in ^{42}Ar.

3 Results and discussion

For convenience we report in Fig. 1 the partial level scheme of ^{40,41,42}Ar, pertinent for the present discussion of the $E2$ transitions, with the energy, spin, parity of the states, and the energy of transitions as in Ref. [2]. We briefly remind that these states were discussed in terms of the sd−pf large-scale shell-model (SM) calculations [24,25] by using the SDPF-U effective interaction, with the valence space of the full sd shell for the protons and the full pf shell for the neutrons. The dominant configuration of the 0^+ and 2^+ states in the even Ar isotopes were with two and four neutrons in $f_{7/2}$ for ^{40}Ar and ^{42}Ar, respectively, with the $(d_{5/2})^6(s_{1/2})^2(d_{3/2})^2$ proton configuration. This proton configuration amounts to 75% and 55% for the 0^+ state, and to 71% and 49% for the 2^+ state in ^{40}Ar and ^{42}Ar, respectively. With the addition of neutrons a

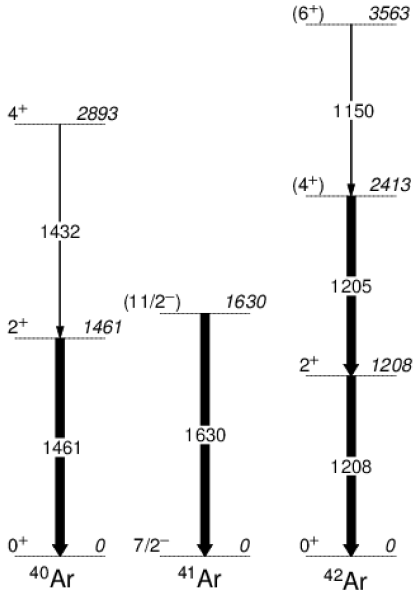

Fig. 1. Experimental level schemes of ^{40}Ar (left), ^{41}Ar (middle) and ^{42}Ar (right), showing only the transitions relevant for the angular distribution analysis. Relative γ-ray intensities are indicated by the width of the arrows. The energy, spin, parity of levels, and the energy of the transitions, are as in Refs. [2,23].

single $s_{1/2}$ proton is promoted to the $d_{3/2}$ orbital, and this depletion of $s_{1/2}$ strongly contributes to the increase of collectivity. The $7/2^-$ ground state of ^{41}Ar was well described by a neutron in the $f_{7/2}$ orbital, with a large part of its wave function which can be understood as $0^+ \otimes \nu f_{7/2}$ configuration. We also found a large concentration of 2^+ of ^{40}Ar coupled to the neutron in $f_{7/2}$ in the $(11/2^-)$ state.

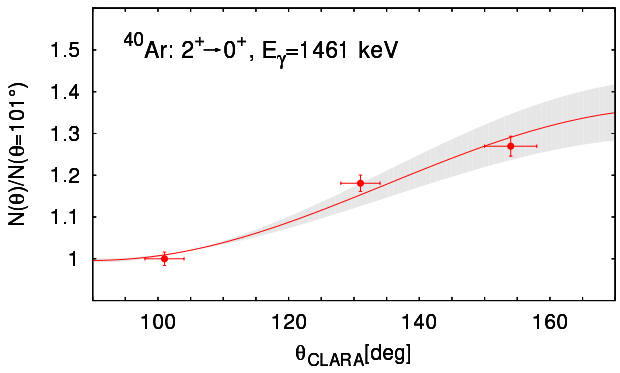

Fig. 2. (Color online): Angular distribution of the 1461 keV $2^+ \rightarrow 0^+$ transition in ^{40}Ar (points). The errors in the ratio $N(\theta)/N(\theta = 101^\circ)$ are only statistical, those in $\theta_{\rm CLARA}$ correspond to the angular range defined by the detector geometry. The curve is a fit with the function $W(\theta) = a_0(1 + a_2 P_2)$, with $a = a_0 \times a_2 = 0.25$. The shaded area represents the overall uncertainty of the fit.

We start the analysis by showing the angular distribution for the $2^+ \rightarrow 0^+$ quadrupole transition in ^{40}Ar. This well known transition of $E2$ character is taken as reference to test the validity and sensitivity of the adopted method. The experimental angular distribution is plotted in Fig. 2. In the same figure we report the results of the fitting procedure with the $W(\theta)$ function where the shaded area represents the uncertainty of the fit. From the fit we extracted a coefficient $a = 0.25$ (see also table Tab. 1). The value calculated by assuming a stretched quadrupole $2^+ \rightarrow 0^+$ transition and taking into account a maximum spin alignment turns out to be $a_{max} = 0.71$. In this entrance channel mass partition the largest contribution to the excitation of the 2^+ state is due to Coulomb excitation. We thus expect a certain level of alignment, compatible with the observed ratio a/a_{max}, representing the attenuation coefficient.

The experimental a values, for this and other Ar isotopes, are reported in Tab. 1, together with additional relevant information. We also report the intensity ratio at "small" (close to 90°) and "large" (close to 180°) angle, which is a useful parameter for a rough estimation of the electromagnetic transition anisotropy. Due to the CLARA geometry we defined this ratio as $R_I = I(154^\circ)/I(101^\circ)$.

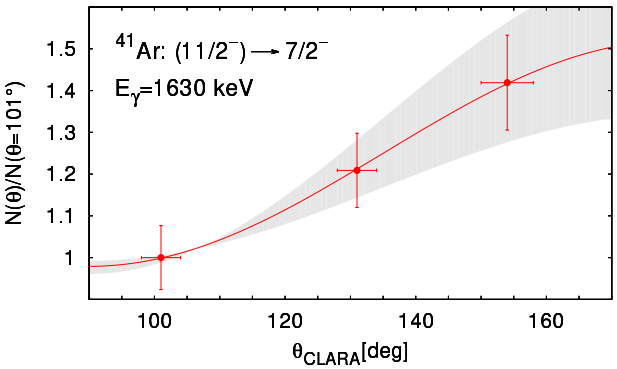

Fig. 3. (Color online): Angular distribution of the 1630 keV $(11/2^-) \rightarrow 7/2^-$ transition in ^{41}Ar. Errors and shaded area are defined as in Fig. 2. The red curve is a fit with the function $W(\theta)$ with $a = 0.3$.

Following the outlined procedure, we constructed the angular distribution for the 1630 keV photo-peak in ^{41}Ar, which was attributed to the $(11/2^-) \rightarrow 7/2^-$ transition [2]. The results are shown in Fig. 3. The curve is the $W(\theta)$ fit, from which one obtains $a = (0.3 \pm 0.1)$, to be compared with the calculated one a_{max}=0.45 expected for a stretched quadrupole transition from the fully aligned $11/2^-$ spin. The attenuation coefficient of 0.67 indicates a high level of alignment in this one-neutron transfer channel. This attenuation coefficient is plotted in Fig. 4, together with the coefficients of other transitions here studied (full/red symbols). In the same figure we chose to plot, also, the results of the known $E2$ transitions populated in the ^{48}Ca+^{208}Pb reaction [26]. We would like to stress that these reported states have been populated by transfer reactions, using the same ^{208}Pb target and a similar incident energy as in our ^{40}Ar+^{208}Pb case. Both reactions have been measured with the PRISMA-CLARA set-up, where the reaction plane is well defined by the PRISMA spec-

Isotope	E_γ [keV]	$J_f^\pi \rightarrow J_i^\pi$	Mult.	a	R_I
^{40}Ar	1461	$2^+ \rightarrow 0^+$	$E2$	0.25±0.05	1.3±0.1
	1432	$4^+ \rightarrow 2^+$	$E2$	0.4±0.1	1.4±0.1
^{41}Ar	1630	$(11/2^-) \rightarrow 7/2^-$	$(E2)$	0.3±0.1	1.4±0.1
^{42}Ar	1208,1205	$2^+ \rightarrow 0^+$, $(4^+) \rightarrow 2^+$	$E2$, $(E2)$	0.44±0.05	1.5±0.1
	1150	$(6^+) \rightarrow (4^+)$	$(E2)$	1.4±0.4	2.6±0.4

Table 1. γ ray energy, spin, parity, multipolarity, $a = a_0 \times a_2$ and R_I coefficients for the transitions of ^{40,41,42}Ar considered in the present work. The R_I ratio is defined as $R_I = I(154°)/I(101°)$ (see text). E_γ, J_f^π and J_i^π are as in Ref. [2]. Known multipolarities are as in Ref. [23] while those deduced in the present work are labelled as $(E2)$.

trometer. Similar average values for the alignment were previously reported for $E2$ transitions in Ca isotopes [6] populated in the ^{48}Ca+^{64}Ni transfer reactions.

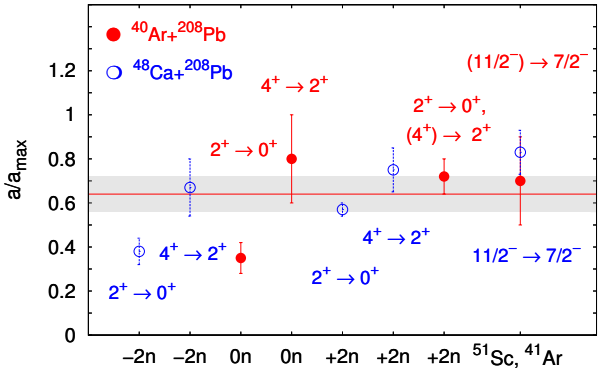

Fig. 4. (Color online): The attenuation coefficient, $a/a_{\max}$, for the indicated transitions in the $(-2n)$ (^{46}Ca) and $(+2n)$ (^{50}Ca) channels in the ^{48}Ca+^{208}Pb reaction (blue/empty symbols) [26], are plotted together with coefficients obtained in the present work (red/full symbols) for the ^{40}Ar+^{208}Pb reaction. The average attenuation coefficient (0.64±0.08) of ^{40}Ar+^{208}Pb is indicated by the red-full line with the shaded area uncertainties. The $11/2^- \rightarrow 7/2^-$ transitions in ^{51}Sc populated in the ^{48}Ca+^{208}Pb reaction via the $(+1p+2n)$ channel, and in ^{41}Ar populated in ^{40}Ar+^{208}Pb via $(+1n)$, are included.

As a follow up of the presented analysis of the $E2$ transitions in ^{40,41}Ar, we applied the same procedure also for ^{42}Ar. We would like to remind that the γ rays of the transitions $2^+ \rightarrow 0^+$ and $(4^+) \rightarrow 2^+$ in ^{42}Ar have very similar energies [2]. They have been extracted from particle-γ-γ spectra as 1208 and 1205 keV, respectively. Unfortunately, due to the limited statistics of our experiment, the two transitions could not be analyzed separately, and the angular distribution has been constructed by integrating the whole doublet (top panel of Fig. 5). Nevertheless, the summed angular distribution for the two transitions is compatible with the quadrupole nature of both of them, once the attenuation factor is taken into account.

In the bottom panel of the same figure we plot the angular distribution for the $(6^+) \rightarrow (4^+)$ transition, where the large errors, reflecting the limited statistics, lead to significant uncertainties in the fitting procedure and a rather large a value. For completeness, we also added in

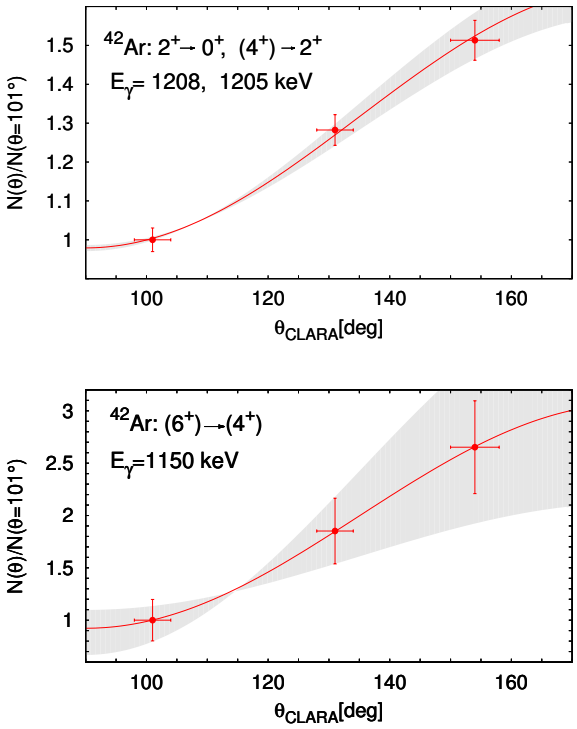

Fig. 5. (Color online): Angular distribution in ^{42}Ar for the 1208(+1205) keV photo-peak attributed to $(4^+) \rightarrow 2^+$ and $2^+ \rightarrow 0^+$ (top), and for the 1150 keV $(6^+) \rightarrow (4^+)$ transition (bottom). Errors and shaded area are defined as in Fig. 2. The red curves are fits with the $W(\theta)$ function.

Tab. 1 the results for the $4^+ \rightarrow 2^+$ established $E2$ transition in ^{40}Ar. Attenuation coefficients of these transitions are also plotted in Fig. 4.

Due to the CLARA geometry, the analyzed angular distributions incorporate a limited (actually three) number of experimental points. In spite of this limitation, all distributions turn out to be compatible with a quadrupole character. The analysed transitions exhibit a large amount of spin alignment, about ∼70% for pure transfer channels. In particular, the 1630 keV transition in ^{41}Ar displays an angular distribution of quadrupole character and therefore the excited state at 1630 keV is consistent with a $11/2^-$ state. These findings well agree with the attribution of a dominant $2^+ \otimes \nu f_{7/2}$ stretched configuration to the $11/2^-$ state.

In the recent work [26] the structure of the neutron rich Ca isotopes, in particular the ^{49}Ca and ^{47}Ca nuclei populated in the one-neutron transfer channels, were investigated via γ ray angular distributions, with additional information from life-time measurements. A strong excitation of the $9/2^+$ state in ^{49}Ca and $11/2^+$ state in ^{47}Ca was observed, and their structure interpreted as a particle/hole coupled to the 3^- phonon of ^{48}Ca [6, 26, 27]. Such interpretation in terms of a phonon-fermion coupling scheme came also from the very recent work of Ref. [8], where the level structure of the neutron rich ^{39}S has been studied in the ^{36}S+^{208}Pb reaction, measured with the same PRISMA+CLARA set-up. In particular, a γ transition of 1517 keV was attributed to the decay of the $11/2^-$ state to the ground state, similarly to our ^{41}Ar isotone case. The analysis supports the structure of this state in ^{39}S as due to the unpaired neutron in the $f_{7/2}$ orbital coupled to the 2^+ of the ^{38}S core. This fact was used to systematically study the behaviour of the excitation energy difference $E(11/2^-) - E(7/2^-)$ in odd-S isotopes in order to follow the quadrupole deformation in neutron rich sulfur isotopes.

4 Summary

We analyzed the γ angular distributions for selected transitions in ^{40,41,42}Ar isotopes. These isotopes have been populated in the ^{40}Ar+^{208}Pb inelastic and transfer reactions making use of the PRISMA spectrometer coupled to the CLARA γ array. By exploiting the modularity of CLARA, the angular distributions of the strong transitions have been constructed, allowing to establish more firmly the spin and parity of populated states. To this aim, we also took advantage of the high level of spin alignment in the neutron transfer channels. In particular, through the study of the 1630 keV transition, the structure of the $(11/2^-)$ state in ^{41}Ar has been described as a stretched configuration of the $f_{7/2}$ valence neutron coupled to the 2^+ vibration phonon. Such results support the importance of phonon-fermion coupling in the description of the states populated via nucleon transfer.

5 Acknowledgement

The authors are grateful to the LNL Tandem-ALPI staff for the good quality beams and the target laboratory for the excellent targets. This work was partly supported by the EC FP7 Contract ENSAR (262010). This work has been supported in part by the Croatian Science Foundation under the project 7194, in part by the Scientific center of excellence for advance materials and sensors in Zagreb. One of the authors (A.G.) has been supported by MINECO, Spain, under the grant FPA2014-57196-C5, Generalitat Valenciana, Spain, under the grant PROMETEOII/2014/019 and EU under the FEDER program.

References

1. A. Bohr, and B.R. Mottelson, *Nuclear Structure*, Vol. II, W.A. Benjamin, Inc., New York, 1975.
2. S. Szilner, L. Corradi, F. Haas, D. Lebhertz, G. Pollarolo, C. A. Ur, L. Angus, S. Beghini, M. Bouhelal, R. Chapman, E. Caurier, S. Courtin, E. Farnea, E. Fioretto, A. Gadea, A. Goasduff, D. Jelavić Malenica, V. Kumar, S. Lunardi, N. Märginean, P. Mason, D. Mengoni, G. Montagnoli, F. Nowacki, F. Recchia, E. Sahin, M.-D. Salsac, F. Scarlassara, R. Silvestri, J. F. Smith, N. Soić, A. M. Stefanini, and J. J. Valiente-Dobón, Phys. Rev. C **84**, 014325 (2011).
3. S. Lunardi, S. M. Lenzi, F. Della Vedova, E. Farnea, A. Gadea, N. Märginean, D. Bazzacco, S. Beghini, P. G. Bizzeti, A. M. Bizzeti-Sona, D. Bucurescu, L. Corradi, A. N. Deacon, G. de Angelis, E. Fioretto, S. J. Freeman, M. Ionescu-Bujor, A. Iordachescu, P. Mason, D. Mengoni, G. Montagnoli, D. R. Napoli, F. Nowacki, R. Orlandi, G. Pollarolo, F. Recchia, F. Scarlassara, J. F. Smith, A. M. Stefanini, S. Szilner, C. A. Ur, J. J. Valiente-Dobón, and B. J. Varley, Phys. Rev. C **76**, 034303 (2007).
4. J. J. Valiente-Dobón, D. Mengoni, A. Gadea, E. Farnea, S. M. Lenzi, S. Lunardi, A. Dewald, Th. Pissulla, S. Szilner, R. Broda, F. Recchia, A. Algora, L. Angus, D. Bazzacco, G. Benzoni, P. G. Bizzeti, A. M. Bizzeti-Sona, P. Boutachkov, L. Corradi, F. Crespi, G. de Angelis, E. Fioretto, A. Gorgen, M. Gorska, A. Gottardo, E. Grodner, B. Guiot, A. Howard, W. Krolas, S. Leoni, P. Mason, R. Menegazzo, D. Montanari, G. Montagnoli, D. R. Napoli, A. Obertelli, T. Pawlat, B. Rubio, E. Sahin, F. Scarlassara, R. Silvestri, A. M. Stefanini, J. F. Smith, D. Steppenbeck, C. A. Ur, P. T. Wady, J. Wrzesinski, E. Maglione, and I. Hamamoto, Phys. Rev. Lett. **102**, 242502 (2009).
5. D. Mengoni, J.J. Valiente-Dobón, A. Gadea, S. Lunardi, S. M. Lenzi, R. Broda, A. Dewald, T. Pissulla, L. J. Angus, S. Aydin, D. Bazzacco, G. Benzoni, P. G. Bizzeti, A. M. Bizzeti-Sona, P. Boutachkov, L. Corradi, F. Crespi, G. de Angelis, E. Farnea, E. Fioretto, A. Goergen, M. Gorska, A. Gottardo, E. Grodner, A. M. Howard, W. Królas, S. Leoni, P. Mason, D. Montanari, G. Montagnoli, D. R. Napoli, A. Obertelli, R. Orlandi, T. Pawlat, G. Pollarolo, F. Recchia, A. Algora, B. Rubio, E. Sahin, F. Scarlassara, R. Silvestri, J. F. Smith, A. M. Stefanini, D. Steppenbeck, S. Szilner, C. A. Ur, P. T. Wady, and J. Wrzesiński, Phys. Rev. C **82**, 024308 (2010).
6. D. Montanari, S. Leoni, D. Mengoni, G. Benzoni, N. Blasi, G. Bocchi, P. F. Bortignon, A. Bracco, F. Camera, G. Coló, A. Corsi, F. C. L. Crespi, B. Million, R. Nicolini, O. Wieland, J. J. Valiente-Dobón, L. Corradi, G. de Angelis, F. Della Vedova, E. Fioretto, A. Gadea, D. R. Napoli, R. Orlandi, F. Recchia, E. Sahin, R. Silvestri, A. M. Stefanini, R. P. Singh, S. Szilner, D. Bazzacco, E. Farnea, R. Menegazzo, A. Gottardo, S. M. Lenzi, S. Lunardi, G. Montagnoli, F. Scarlassara, C. A. Ur, G. Lo Bianco, A. Zucchiatti, M. Kmiecik, A. Maj, W. Meczynski, A. Dewald, Th. Pissulla, and G. Pollarolo, Phys. Lett. B **697**, 288 (2011).
7. S. Szilner, L. Corradi, F. Haas, G. Pollarolo, L. Angus, S. Beghini, M. Bouhelal, R. Chapman, E. Caurier, S. Courtin, E. Farnea, E. Fioretto, A. Gadea, A. Goasduff, D. Jelavić Malenica, V. Kumar, S. Lunardi, N. Märginean, D. Mengoni, T. Mijatović, G. Montagnoli, F. Recchia, E. Sahin, M.-D. Salsac, F. Scarlassara, J. F. Smith, N. Soić, A. M. Stefanini, C. A. Ur, and J. J. Valiente-Dobón, Phys. Rev. C **87**, 054322 (2013).

8. R. Chapman, Z. M. Wang, M. Bouhelal, F. Haas, X. Liang, F. Azaiez, B. R. Behera, M. Burns, E. Caurier, L. Corradi, D. Curien, A. N. Deacon, Zs. Dombradi, E. Farnea, E. Fioretto, A. Gadea, A. Hodsdon, F. Ibrahim, A. Jungclaus, K. Keyes, V. Kumar, S. Lunardi, N. Marginean, G. Montagnoli, D. R. Napoli, F. Nowacki, J. Ollier, D. ODonnell, A. Papenberg, G. Pollarolo, M.-D. Salsac, F. Scarlassara, J. F. Smith, K. M. Spohr, M. Stanoiu, A. M. Stefanini, S. Szilner, M. Trotta, and D. Verney, Phys. Rev. C **94**, 024325 (2016).
9. P. J. A. Buttle, and L. J. B. Goldfarb, Nucl.Phys. A **176**, 299 (1971).
10. D. M. Brink, Phys. Lett. B **40**, 37 (1972).
11. L. Corradi, G. Pollarolo and S. Szilner, J. of Phys. G **36**, 113101 (2009).
12. T. Mijatović, S. Szilner, L. Corradi, D. Montanari, G. Pollarolo, E. Fioretto, A. Gadea, A. Goasduff, D. Jelavić Malenica, N. Mărginean, M. Milin, G. Montagnoli, F. Scarlassara, N. Soić, A. M. Stefanini, C. A. Ur, and J. J. Valiente-Dobón, Phys. Rev. C **94**, 064616 (2016).
13. T. Mijatović, S. Szilner, L. Corradi, D. Montanari, G. Pollarolo, E. Fioretto, A. Gadea, A. Goasduff, D. Jelavić Malenica, N. Mărginean, G. Montagnoli, F. Scarlassara, N. Soić, A. M. Stefanini, C. A. Ur, and J. J. Valiente-Dobón, Eur. Phys. J. A **52**, 113 (2016).
14. A. M. Stefanini, L. Corradi, G. Maron, A. Pisent, M. Trotta, A. M. Vinodkumar, S. Beghini, G. Montagnoli, F. Scarlassara, G. F. Segato, A. De Rosa, G. Inglima, D. Pierroutsakou, M. Romoli, M. Sandoli, G. Pollarolo, and A. Latina, Nucl. Phys. **A701**, 217c (2002).
15. S. Szilner, C. A. Ur, L. Corradi, N. Mărginean, G. Pollarolo, A. M. Stefanini, S. Beghini, B. R. Behera, E. Fioretto, A. Gadea, B. Guiot, A. Latina, P. Mason, G. Montagnoli, F. Scarlassara, M. Trotta, G. de Angelis, F. Della Vedova, E. Farnea, F. Haas, S. Lenzi, S. Lunardi, R. Marginean, R. Menegazzo, D. R. Napoli, M. Nespolo, I. V. Pokrovsky, F. Recchia, M. Romoli, M.-D. Salsac, N. Soić, and J. J. Valiente-Dobón, Phys. Rev. C **76**, 024604 (2007).
16. L. Corradi, S. Szilner, G. Pollarolo, D. Montanari, E. Fioretto, A. Stefanini, J. Valiente-Dobón, E. Farnea, C. Michelagnoli, G. Montagnoli, F. Scarlassara, C. Ur, T. Mijatović, D. J. Malenica, N. Soić, and F. Haas, Nucl. Instr. and Meth. in Phys. Res. B **317**, 743 (2013).
17. A. Gadea, D. R. Napoli, G. de Angelis, R. Menegazzo, A. M. Stefanini, L. Corradi, M. Axiotis, L. Berti, E. Fioretto, T. Kroell, A. Latina, N. Marginean, G. Maron, T. Martinez, D. Rosso, C. Rusu, N. Toniolo, S. Szilner, M. Trotta, D. Bazzacco, S. Beghini, M. Bellato, F. Brandolini, E. Farnea, R. Isocrate, S. M. Lenzi, S. Lunardi, G. Montagnoli, P. Pavan, C. Rossi Alvarez, F. Scarlassara, C. Ur, N. Blasi, A. Bracco, F. Camera, S. Leoni, B. Million, M. Pignanelli, G. Pollarolo, A. DeRosa, G. Inglima, M. La Commara, G. La Rana, D. Pierroutsakou, M. Romoli, M. Sandoli, P. G. Bizzeti, A. M. Bizzeti-Sona, G. Lo Bianco, C. M. Petrache, A. Zucchiatti, P. Cocconi, B. Quintana, Ch Beck, D. Curien, G. Duchene, F. Haas, P. Medina, P. Papka, J. Durell, S. J. Freeman, A. Smith, B. Varley, K. Fayz, V. Pucknell, J. Simpson, W. Gelletly, P. Regan, The EUROBALL and PRISMA Collaboration, Eur. Phys. J. A **20**, 193 (2004).
18. G. Montagnoli, A.M. Stefanini, M. Trotta, S. Beghini, M. Bettini, F. Scarlassara, V. Schiavon, L. Corradi, B. R. Behera, R. Fioretto, A. Gadea, A. Latina, S. Szilner, L. Donà, M. Rigato, N. A. Kondratiev, A. Yu. Chizhov, G. Kniajeva, E. M. Kozulin, I. V. Pokrovskiy, V. M. Voshressensky, and D. Ackermann, Nucl. Instr. and Meth. in Phys. Res. A **547**, 455 (2005).
19. S. Beghini, L. Corradi, E. Fioretto, A. Gadea, A. Latina, G. Montagnoli, F. Scarlassara, A. M. Stefanini, S. Szilner, M. Trotta, and A. M. Vinodkumar, Nucl. Instr. and Meth. in Phys. Res. A **551**, 364 (2005).
20. D. Montanari, E. Farnea, S. Leoni, G. Pollarolo, L. Corradi, G. Benzoni, E. Fioretto, A. Latina, G. Montagnoli, F. Scarlassara, R. Silvestri, A. M. Stefanini, and S. Szilner, Eur. Phys. J. A **47**, 4 (2011).
21. A. H. Wapstra, G. J. Nijgh, and R. Van Lieshout Nuclear Spectroscopy Tables, North-Holland, Amsterdam, VII (1959).
22. T. Yamazaki, Nucl. Data A **3**, 1 (1967).
23. Nucl. Data Sheets **92**, 783 (2001); **94**, 1 (2001); **94**, 429 (2001); National Nuclear Data Center, http://www.nndc.bnl.gov/.
24. E. Caurier, G. Martínez-Pinedo, F. Nowacki, A. Poves, and A. P. Zuker, Rev. Mod. Phys. **77**, 427 (2005).
25. F. Nowacki, and A. Poves, Phys. Rev. C **79**, 014310 (2009).
26. D. Montanari, S. Leoni, D. Mengoni, J. J. Valiente-Dobón, G. Benzoni, N. Blasi, G. Bocchi, P. F. Bortignon, S. Bottoni, A. Bracco, F. Camera, P. Casati, G. Colò, A. Corsi, F. C. L. Crespi, B. Million, R. Nicolini, O. Wieland, D. Bazzacco, E. Farnea, G. Germogli, A. Gottardo, S. M. Lenzi, S. Lunardi, R. Menegazzo, G. Montagnoli, F. Recchia, F. Scarlassara, C. Ur, L. Corradi, G. de Angelis, E. Fioretto, D. R. Napoli, R. Orlandi, E. Sahin, A. M. Stefanini, R. P. Singh, A. Gadea, S. Szilner, M. Kmiecik, A. Maj, W. Meczynski, A. Dewald, Th. Pissulla, and G. Pollarolo, Phys. Rev. C **85**, 044301 (2012).
27. G. Coló, P. F. Bortignon, and G. Bocchi, Phys. Rev. C **95**, 034303 (2017).